Influence of wave spreading on offshore wind turbine design: IEA 15-MW scenario

Journal of Physics: Conference Series **2767** (2024) 062028 doi:10.1088/1742-6596/2767/6/062028

Influence of wave spreading on offshore wind turbine design: IEA 15-MW scenario

Gerard V. Ryan[1], **Ross A. McAdam**[2] **and Thomas A. A. Adcock**[1]

[1]Department of Engineering Science, University of Oxford, Oxford, UK
[2]Department of Geotechnical Design, Ørsted Wind Power, London, UK

E-mail: gerard.ryan@eng.ox.ac.uk

Abstract. Offshore ocean waves are directionally spread, whereby the propagation of energy travels in different directions. Despite this multi-directionality, the use of 3-dimensional wave models for loading on fixed offshore wind turbines has been limited. This is partially due to the common assumption that uni-directional sea-states are conservative within a design philosophy. This may not always be true given that in operating conditions the amount of aerodynamic damping in the side-side direction is much lower than the fore-aft direction. This paper aims to address this issue by providing the influence of wave spreading on various offshore wind turbine design scenarios: fatigue, ultimate and service limit state design. This study demonstrates that wave spreading indeed results in more fatigue damage for operating load cases. Despite this, the overall fatigue and ultimate limit state utilisation is still reduced when a wave spreading is adopted.

1 Introduction

The dynamic behaviour of an offshore wind turbine (OWT), which is a key driver of the material cost for the structure, is heavily dependent on the damping of the system and loading at the structural natural frequencies. During operating conditions, the alteration of the rotor aerodynamic forces due to tower top motion provides most of the tower and monopile fore-aft damping [1, 2]. This interaction also occurs in the side-to-side direction, however the influence is much lower, meaning that the overall damping in this direction is significantly lower than the fore-aft direction [1, 2]. In shallow water depths, wave refraction causes nearshore wave crests to align with seabed contours. However, in intermediate water depths, which are relevant for current offshore wind farm projects [3], waves that are generated locally by wind are typically directionally spread. This directional spreading means that wave loading components are not always in-line with the rotor thrust force that produces significant aerodynamic damping. This may mean that the inclusion of multi-directional wave loading that act in directions with lower damping levels could be more damaging to the structure than the common uni-directional assumption. This is particularly evident for fatigue limit state (FLS) design whereby the damage is calculated as the cumulative effect at various hotspot points around the circumference of the support structure, e.g., monopile foundation. Indeed, Sørum et al. [4] has found that the two most influential parameters for monopile design are wave spreading and the choice of soil model, while acknowledging that wave spreading in particular has received little attention within the research community. Sørum et al. [4] investigated the influence spreading has on FLS design. However, they did not consider any ULS or SLS design and used a frequency independent spreading model. Analysis of field data suggests that the directional spreading is instead frequency-dependent [5]; the peak of the wave spectrum being less

spread, when compared to the high frequency tail. For a sea state characterised by a spectral peak frequency (f_p), the amount of directional spreading at a structural natural frequency (f_n) is dependent on the f_n/f_p ratio. Depending on the spectral peak frequency of interest, the amount of directional spreading at f_n will therefore vary. This is particularly important for FLS, as it is dominated by the response at 1st tower modal frequency. Hence, to accurately capture the variation in directional spreading across a range of sea state scenarios, and therefore loading at the 1st tower modal frequency, requires a frequency dependent spreading model as opposed to a frequency independent model. The objective of this paper is therefore to quantify the influence of frequency dependent wave spreading on FLS, ULS and SLS design of the monopile supported DTU 10 MW turbine. Where the ULS and SLS event is characterised by an extreme storm event with a return period of 50 years (DLC 6.1) [6].

2 Methodology

2.1 Offshore wind turbine model

The turbine used for this study is the IEA 15-MW turbine [7]. The reference site for this study was chosen to represent a typical location in the North Sea, and the assumed metocean data is summarised by in Table 1. The soil conditions consist of a homogeneous over consolidated clay that match the Cowden profile described in Byrne et al. [8].

Table 1: Site metocean data.

Parameters	Values
Mean water depth	45 m
Mean wind speed at mean sea level	8 m/s
Extreme 50-year significant wave height	11.5 m
Extreme 50-year spectral peak period	14.7 s
Extreme 50-year wind speed at hub height	45 m/s

2.2 Aeroelastic tool

To conduct this study, we use our in-house aero-hydro-servo-elastic code [9] which has been verified against industry standard software such as OpenFAST and BLADED. This tool is based in on a multi-body formulation method that is fully coupled with 1-D finite elements, allowing accurate modelling of wind turbines in both operating and parked conditions [9]. Importantly, it enables modelling of the directional dependence of aerodynamic damping through explicitly capturing the aeroelastic behaviour. The stochastic wind field is modelled using the Kaimal spectrum, as described in IEC 61400-3-1[6]. Soil-structure interaction is modelled using a multi-surface plasticity approach capturing soil hysteretic behaviour along the full embedment depth, whereby hysteretic damping is explicitly captured within the mechanics of the model [9]. This being a key reason why we use this code over other software.

2.3 Hydrodynamic modelling

The most common method to calculate hydrodynamic forces on a fixed offshore structure is Morison's equation [10]. In applying Morison's equation, calculations are performed using the undisturbed incident wave field. In the case of recent OWT monopiles installations, the diameter is large enough (8 m-10 m) to disturb the incident flow for common sea-state conditions. This occurs when the diameter divided by incident wavelength exceeds approximately 0.2. Within the present study, we use Morison's equation with the MacCamy and Fuchs correction for fatigue analysis. Wave-structure interaction for extreme waves is inherently non-linear and difficult to predict analytically, despite various formulations which extend the basic linear inertia calculation [11, 12, 13]. An alternative is to infer the non-linear loading experimentally. We use the experimental approach based on the work of Tang et al. [14]. This Stoke-type force model makes the assumption that the non-linear loads are higher harmonics of the primary linear loading, which can be found from a standard linear calculation. This approach builds on the work of [15, 16, 17]. Thus, the forces on the column have the form:

$$F = \hat{\mathcal{F}}_1 \cos(\varphi) + \hat{\mathcal{F}}_1^2 F_2 \cos(2\varphi + \Phi_2) + \hat{\mathcal{F}}_1^3 F_3 \cos(3\varphi + \Phi_3) + \hat{\mathcal{F}}_1^4 F_4 \cos(4\varphi + \Phi_4) + O\left(\hat{\mathcal{F}}_1^5\right) \quad (1)$$

where $\mathcal{F}_1$ is the envelope of the linear force, φ is the phase of the higher order harmonics, which can be obtained from the signal and its Hilbert transform. F_n represents the amplitude coefficients for the nth order of force harmonics and Φ_n is the phase coefficients for the nth order of force. These coefficients are inferred using machine learning from experimental data. Experiments have been designed so that they cover the space relevant for design of offshore wind turbines at present. This model has the key advantages over non-linear analytical methods in that it has negligible computational time and robust to apply given that the primary input is based on linear loading [14], which can easily calculated for each frequency component as:

$$F_1 = \rho g \pi C_m A R^2 \tanh(kd) \cos(\omega t + \alpha), \tag{2}$$

where F_1 is the total linear in-line inertia force integrated to still water level (SWL), ρ the fluid density, g the acceleration due to gravity, C_m the inertia coefficient, A the wave amplitude, R the cylinder radius, k the wave number, d the water depth, ω the angular wave frequency and α is the phase angle. The method is based on an extensive experimental campaign, therefore it is expected to include most of the dominant physical processes and is not restricted by flow field assumptions that are commonly used within analytical models. These analytical assumptions inherently limit the applicability of these analytical models when compared to real wave loading events, as shown in the work by Tromans et al. [18]. We do not consider here the physics from strongly non-linear processes such as wave breaking [19] or secondary load cycles [20, 21].The implementation of the Stokes-GP model, involves using Equation 2 to generate the non-linear wave loads. These are then applied as point loads at still water level, except for the 2nd-order harmonic component, which is applied at 90% of the mean water depth above the seabed [17]. Distributed forces, such as 1st order inertia and drag, are applied using Morison's equation based on a linear kinematic wave field. For the extreme sea state considered, the Keulegan-Carpenter number is less than 5 and linear diffraction has been found to be insignificant, therefore $C_m = 2$ is assumed.

2.4 Short-crested wave fields

In this work, we generate multi-directional wave fields from a 2-D spectrum, as illustrated by Figure 1, which is the product of the 1-D frequency density spectrum given in the JONSWAP form; and a directional spreading function (H) which describes the spread of wave energy in different propagation directions (θ) relative to a mean wave direction (θ_m). Within the present study, Ewans frequency-dependent directional spreading model has been adopted [22] as given below:

$$H(f,\theta) = \frac{1}{\sigma\sqrt{8\pi}} \sum_{j=-\infty}^{\infty} \left\{ \exp\left[-\frac{1}{2} \left(\frac{\theta - \theta_1 - 2\pi j}{\sigma} \right)^2 \right] + \exp\left[-\frac{1}{2} \left(\frac{\theta - \theta_2 - 2\pi j}{\sigma} \right)^2 \right], \tag{3}$$

where

$$\theta_1(f) = \frac{\theta_m + \Delta\theta}{2}, \quad \theta_2(f) = \frac{\theta_m - \Delta\theta}{2}, \tag{4}$$

$$\Delta\theta(f) = \begin{cases} 14.93 \text{ for } f < f_p \\ \exp\left[5.453 - 2.750 \left(\frac{f}{f_p} \right)^{-1} \right] \text{ for } f \geq f_p \end{cases}, \tag{5}$$

$$\sigma(f) = \begin{cases} 11.38 + 5.357 \left(\frac{f}{f_p} \right)^{-7.929} & \text{for } f < f_p \\ 32.13 - 15.39 \left(\frac{f}{f_p} \right)^{-2} & \text{for } f \geq f_p \end{cases}. \tag{6}$$

Within this model, the spreading at the spectral peak is defined by a standard deviation (σ) of approximately 17°, whilst the tail of the wave spectrum is characterised by a standard deviation of approximately 30°. To use this frequency-dependent directional spreading model with the Stokes-GP model (extreme conditions), we use an inline wave kinematic factor. This factor is commonly used to reduce the in-line kinematics (velocities and accelerations) of uni-directional wave theories to account for directionality. Results from [23] has shown that for inertia dominated surface piercing columns, the

harmonic components of the force signal scale with this inline wave kinematic factor to the power of n-th harmonic as given below:

$$\phi_n = \cos(\sigma_\theta)^n, \tag{7}$$

where σ_θ is a representative standard deviation of spreading angle and ϕ_n is the factor to reduce the n-th harmonic loading. We note this is an experimentally derived result based on a single set of test, so should be treated with caution (see also [24]). Higher harmonic loads will therefore be relatively smaller in magnitude for directionally spread seas compared to uni-directional ones. To determine a representative standard deviation of spreading angle we combine the spreading function and the JONSWAP spectrum to obtain a weighted average value as follows:

$$\bar{\sigma} = \frac{1}{\sigma_\eta^2} \int_0^\infty \int_{-\pi}^{\pi} S(\omega) \cdot H(\omega, \theta) \cdot \sigma_\theta(\omega) \cdot \mathrm{d}\theta \cdot \mathrm{d}\omega. \tag{8}$$

For the extreme sea-state conditions given in Table 1, this approximately results in a representative spreading angle standard deviation of 24° and subsequent inline wave kinematic factor of 0.91. We do not consider the small reduction in spreading that can occur under an extreme wave due to non-linear wave-wave interactions [25, 26, 27, 28].

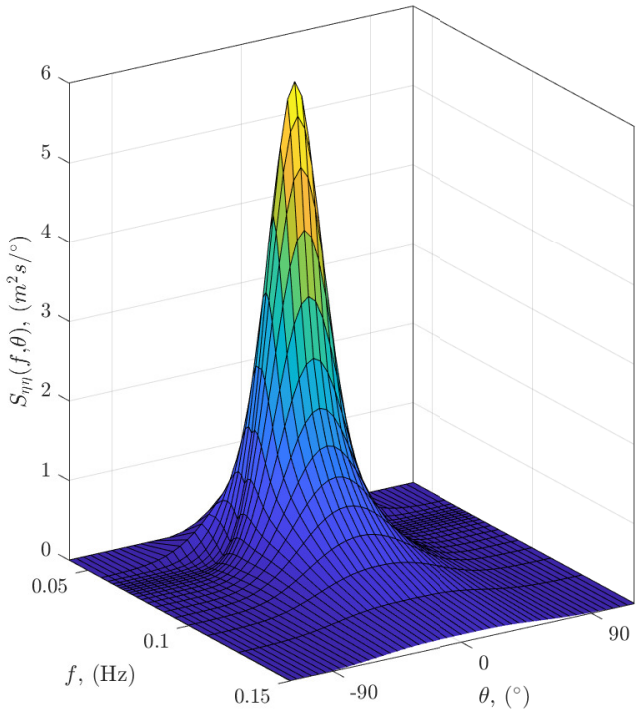

Figure 1: 2-D JONSWAP spectrum with frequency dependent spreading.

2.5 FLS Design checks

The purpose of the fatigue analysis is to verify the resistance of the support structure to cyclic loading in accordance with DNVGL-ST-0126 [29] and DNVGL-RP-C203 [30]. Within the present study, type D S-N curves associated with circumferential welds have been selected along with an SCF of 1.1. The turbine design life is assumed to be 30 years, with 10% of the design life assumed to consist of idling. To conduct the analysis we use over 1200 load cases consisting of wind speeds varying from 3 m/s to 29 m/s, different mean wind direction-mean wave direction misalignment scenarios and turbine modes i.e., idling and operating. Furthermore, for the multi-directional scenario we simulate a kinematics in x, y and z directions.

2.6 ULS Design checks

The purpose of ULS analysis is to verify structural and geotechnical resistance to extreme loading. For primary steel members, this involves yield and stability (local and global buckling) checks undertaken in accordance with DNVGL-ST-0126 [29] and DNGL-RP-C202 [31]. Design load case 6.1 [29] has been analysed, as this typically results in the largest foundation loads an OWT will experience. This load case consists of the largest storm expected to hit the structure within a 50-year return period. From this design scenario, a push over analysis was conducted to assess foundation stability and permanent rotation after an extreme response (SLS). The ULS design capacity was then determined by applying a partial safety factor of 1.4 to the failure envelope in accordance with EN 1997-1 [32]. ULS design loads for foundation stability were conservatively taken as the max bending moment and max shear force at the seabed during the storm event, even though these two maxima may occur at different times. SLS design loads were calculated from these ULS design loads by dividing by 1.35, to remove the partial load factor. The geotechnical design loads and steel utilisation ratios have been calculated as the average value over the worst eight cases (eight 3-hr seeds) identified from the simulated response time-series.

3 FLS analysis

Figure 2 provides the cumulative fatigue damage at the tower top, interface and seabed associated with each wind speed bin for uni-directional and multi-directional scenarios. Within this figure, the damage is shown for operating, idling and combined load cases, each of which are normalised by the max combined damage for the elevation of interest.

The top row of Figure 2 shows the damage at the tower top, where the damage associated with idling load cases is approximately zero when compared to the operating load cases. This implies that most of the damage at tower top comes from operating aerodynamic loads on the rotor. Conversely, both operating and idling load cases contribute significantly to fatigue damage at the interface (middle row). This suggests that the contribution of bending moment induced from nacelle inertia is much more significant at this elevation, as this is the dominant source of bending for idling scenarios. Similar trends to the interface are also seen at the seabed (bottom row). By comparing the multi-directional results to uni-directional results in Figure 2, it is evident that the spreading effect is more significant for idling load cases. There are a few reasons for this. Firstly, aerodynamic forces are much smaller in idling scenarios, meaning that wave loading has a larger influence. Secondly, spreading has the effect of reducing the resultant wave loading, hence the amount of damage is also reduced.

However, it is interesting to note that for some operating load cases, the damage predicted using the multi-directional wave field is larger than the uni-directional scenario. In these scenarios, the effect of reducing the resultant wave loading is outweighed by the effect of loading at an angle to the fore-aft aerodynamic damping i.e. the multi-directionality of wave loading and variation in damping with direction cause an increase in damage from increases in side-to-side resonance.

Figure 3 illustrates an example total wave force time series with and without directional spreading. Depending on the site and turbine of interest, the effect of including spreading may be more or less pronounced. For example, the results may be sensitive to modelling parameters such as the damping of the system, 1st tower mode displacement at mean sea level and the monopile-soil interaction model. Figure 4 shows the depthwise effect spreading has on the total fatigue damage for operating, idling and combined cases. Evidently, the reduction in damage for idling cases due to a reduction in resultant wave loading when spreading is modelled is approximately 30%. In contrast, for the operating cases, there is approximately a 5-10% increase in fatigue damage when spreading is included. The latter being due to loading at an angle that has a lower damping level than the fore-aft direction. The total effect is shown in the combined scenario, whereby approximately a 5-10% reduction in damage is observed when spreading is included.

4 ULS and SLS analysis

4.1 Steel design checks

Figure 5 shows the DLC 6.1 seed averaged max steel utilisation ratios (URs) [31], for each of directionality scenario discussed in the previous sections. This shows the relative importance of spreading in terms of steel UR, where the differences in loading formulation have a significant influence on the corresponding buckling checks that govern this design. Approximately 10% reductions in steel UR are seen when spreading is included. Given that the contribution to bending moment is primarily

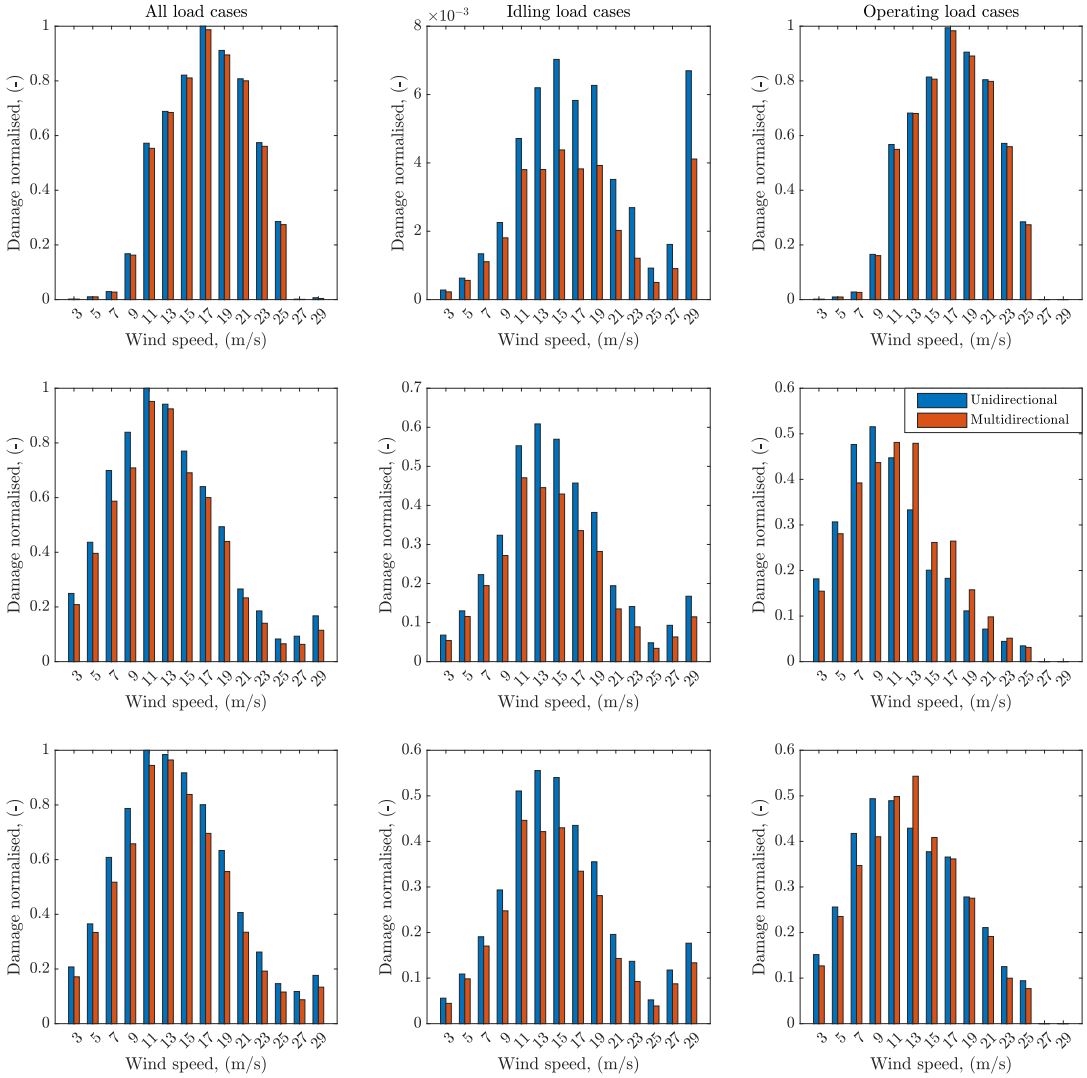

Figure 2: Cumulative fatigue damage at the tower top (top), interface (middle) and seabed (bottom) associated with each wind speed bin for uni-directional and multi-directional scenarios.

due to the nacelle inertia, this decrease in UR is seen from the monopile toe to the top of WTG tower. Hydrodynamic modelling with spreading within a design framework would therefore likely result in a decreased amount of steel required, e.g., decreased monopile wall thickness.

4.2 Geotechnical design checks

Figure 6 shows the SLS and ULS geotechnical design checks, for each directionality scenario discussed in the previous sections. This shows the relative importance of spreading in terms of foundation stability (top) and permanent rotation after an extreme response (bottom). Where the differences in loading formulation again have a significant influence on the corresponding design checks. Approximately 15% reductions in geotechnical utilisation is seen when spreading is included. This would therefore likely result in a further reduction in steel required, e.g., reduced pile embedment depth.

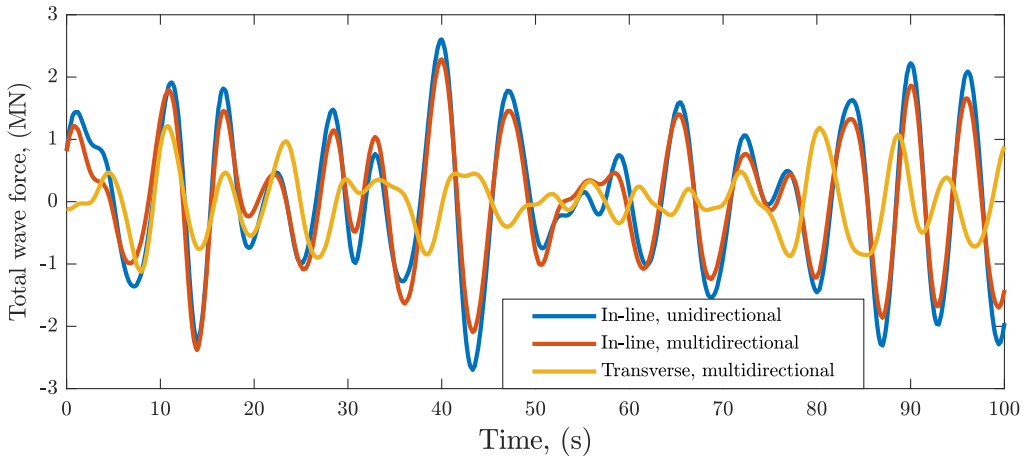

Figure 3: Wave force time series with and without directional spreading.

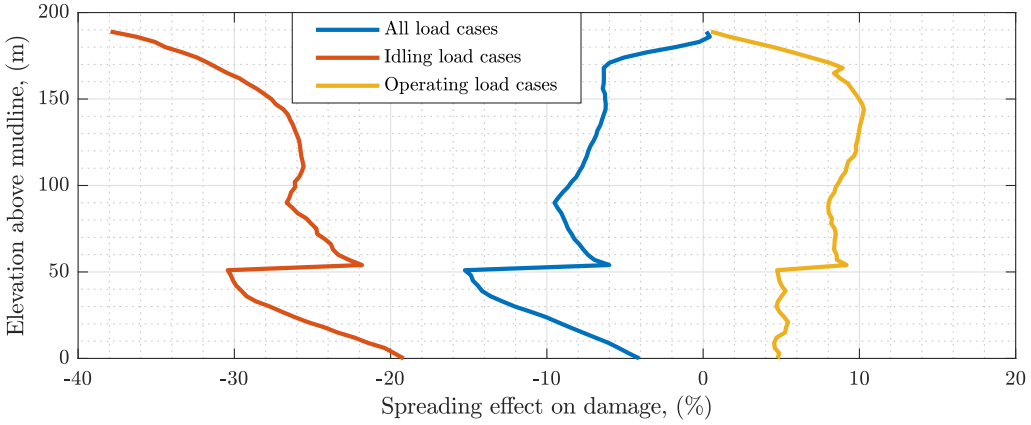

Figure 4: Depth-wise spreading effect on fatigue damage for operating, idling and combined cases.

5 Conclusions

This paper addresses the influence of spreading on the design of a monopile supported IEA 15-MW turbine against fatigue, ultimate and service limit state failure. Namely, that significant reductions in steel and geotechnical UR are observed when spreading is included. The origin of this reduction comes from the decrease in loading magnitude associated with directionally spread seas. Where the reduction is proportional to inline wave kinematic factor to the power of the harmonic order [23]. However, the fatigue analysis also demonstrates that it is non-conservative in operating load cases to assume that sea states are uni-directional, despite being a common design assumption. This non-conservatism deriving from multi-directional loading within directionally spread seas, acting in directions that have lower damping levels than the fore-aft direction. This leads to approximately a 5-10% increase in fatigue damage for the operating cases considered. For idling cases, there is not this strong dependence on direction for damping. Consequently, approximately a 30% reduction in damage is observed for idling scenarios.

Acknowledgments

The authors would like to acknowledge the University of Oxford for funding this work through the Wind and Marine Energy Systems Centre for Doctoral Training. Furthermore, the author would like to thank the SeaSwallows team for making the Stokes-GP model available for use within this paper.

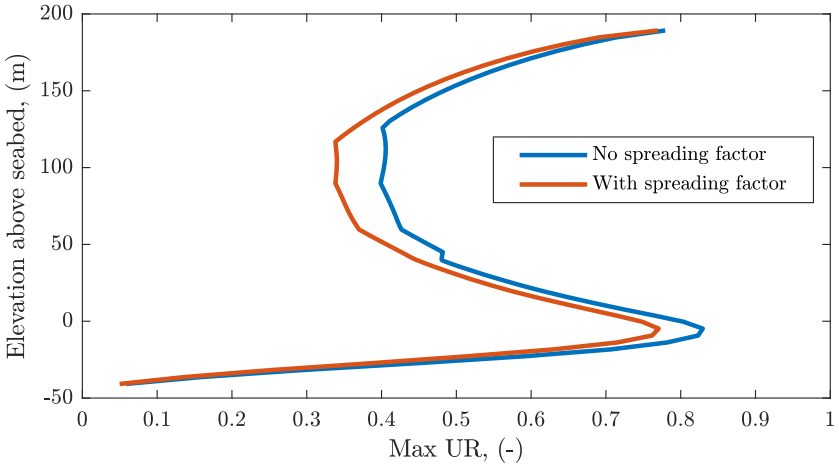

Figure 5: Steel utilisation ratios for each directionality scenario.

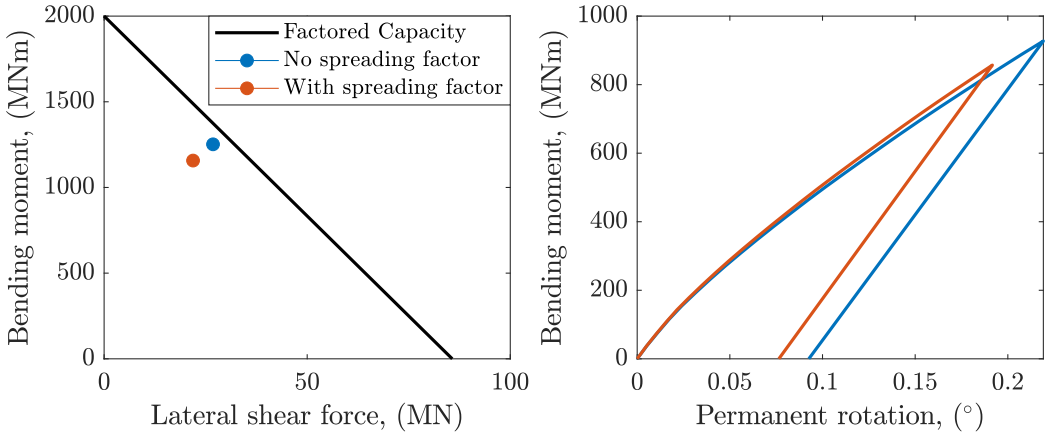

Figure 6: Geotechnical failure envelope / ultimate load interaction diagram for each directionality scenario (left). Rotation at seabed (permanent at unload level) for each directionality scenario (right).

References

[1] Valamanesh, Vahid and Myers, AT. "Aerodynamic damping and seismic response of horizontal axis wind turbine towers." *Journal of Structural Engineering* Vol. 140 No. 11 (2014): p. 04014090.

[2] da Silva Oliveira, Gustavo Miguel Cameira. "Vibration-based structural health monitoring of wind turbines." Ph.D. Thesis, Universidade do Porto (Portugal). 2016.

[3] "Offshore wind in Europe - key trends and statistics 2020. Tech rep." *51st AIAA Aerospace Sciences Meeting including the New Horizons Forum and Aerospace Exposition*: p. 1. 2021. Wind Europe.

[4] Sørum, Stian H, Katsikogiannis, George, Bachynski-Polić, Erin E, Amdahl, Jørgen, Page, Ana M and Klinkvort, Rasmus T. "Fatigue design sensitivities of large monopile offshore wind turbines." *Wind Energy* Vol. 25 No. 10 (2022): pp. 1684–1709.

[5] Mitsuyasu, Hisashi, Tasai, Fukuzo, Suhara, Toshiko, Mizuno, Shinjiro, Ohkusu, Makoto, Honda, Tadao and Rikiishi, Kunio. "Observations of the directional spectrum of ocean WavesUsing a cloverleaf buoy." *Journal of Physical Oceanography* Vol. 5 No. 4 (1975): pp. 750–760.

[6] IEC, IEC/EN. "61400-3-1: 2019 Part 3-1: Design Requirements for Fixed Offshore Wind Turbines." *International Electrotechnical Commission: Geneva, Switzerland* (2019).

[7] Gaertner, Evan, Rinker, Jennifer, Sethuraman, Latha, Zahle, Frederik, Anderson, Benjamin, Barter, Garrett E, Abbas, Nikhar J, Meng, Fanzhong, Bortolotti, Pietro, Skrzypinski, Witold et al. "IEA wind TCP task 37: definition of the IEA 15-megawatt offshore reference wind turbine." Technical report no. National Renewable Energy Lab.(NREL), Golden, CO (United States). 2020.

[8] Byrne, Byron W, McAdam, Ross A, Burd, Harvey J, Beuckelaers, William JAP, Gavin, Kenneth G, Houlsby, Guy T, Igoe, David JP, Jardine, Richard J, Martin, Christopher M, Muir Wood, Alastair et al. "Monotonic laterally loaded pile testing in a stiff glacial clay till at Cowden." *Géotechnique* Vol. 70 No. 11 (2020): pp. 970–985.

[9] Ryan, Gerard V, Adcock, Thomas A A and McAdam, Ross A. "Influence of soil plasticity models on offshore wind turbine response." *Wind Energy* (2023).

[10] Morison, JR, Johnson, Joseph W and Schaaf, Samuel A. "The force exerted by surface waves on piles." *Journal of Petroleum Technology* Vol. 2 No. 05 (1950): pp. 149–154.

[11] Rainey, RCT. "Slender-body expressions for the wave load on offshore structures." *Proceedings of the Royal Society of London. Series A: Mathematical and Physical Sciences* Vol. 450 No. 1939 (1995): pp. 391–416.

[12] Faltinsen, Odd M, Newman, JN and Vinje, T. "Nonlinear wave loads on a slender vertical cylinder." *Journal of Fluid Mechanics* Vol. 289 (1995): pp. 179–198.

[13] Taylor, P H, Tang, T, Adcock, T A A and Zang, J. "Transformed-FNV: wave forces on a vertical cylinder-a free-surface formulation." *Coastal Engineering* (2024).

[14] Tang, Tianning, Ryan, Gerard, Ding, Haoyu, Chen, Xi, Zang, Jun, Taylor, Paul H and Adcock, Thomas A A. "A new Gaussian Process based model for non-linear wave loading on vertical cylinders." *Coastal Engineering* (2023): p. 104427.

[15] Fitzgerald, C J, Taylor, Paul H, Eatock Taylor, R, Grice, J and Zang, J. "Phase manipulation and the harmonic components of ringing forces on a surface-piercing column." *Proceedings of the Royal Society A: Mathematical, Physical and Engineering Sciences* Vol. 470 No. 2168 (2014): p. 20130847.

[16] Chen, L F, Zang, J, Taylor, P H, Sun, L, Morgan, G C J, Grice, J, Orszaghova, J and Tello Ruiz, M. "An experimental decomposition of nonlinear forces on a surface-piercing column: Stokes-type expansions of the force harmonics." *Journal of Fluid Mechanics* Vol. 848 (2018): pp. 42–77.

[17] Feng, X, Taylor, P H, Dai, S, Day, A H, Willden, R H J and Adcock, T A A. "Experimental investigation of higher harmonic wave loads and moments on a vertical cylinder by a phase-manipulation method." *Coastal Engineering* Vol. 160 (2020): p. 103747.

[18] Tromans, P, Swan, C and Masterton, S. "Nonlinear Potential Flow Forcing: the Ringing of Concrete Gravity Based Structures-A Summary Report." Technical report no. HSE Research Report. 2006.

[19] Bredmose, Henrik and Jacobsen, Niels G. "Breaking wave impacts on offshore wind turbine foundations: focused wave groups and CFD." *International Conference on Offshore Mechanics and Arctic Engineering*, Vol. 49118: pp. 397–404. 2010.

[20] Swan, C and Sheikh, R. "The interaction between steep waves and a surface-piercing column." *Philosophical Transactions of the Royal Society A: Mathematical, Physical and Engineering Sciences* Vol. 373 No. 2033 (2015): p. 20140114.

[21] Riise, Bjørn Hervold, Grue, John, Jensen, Atle and Johannessen, Thomas B. "A note on the secondary load cycle for a monopile in irregular deep water waves." *Journal of Fluid Mechanics* Vol. 849 (2018): p. R1.

[22] Ewans, Kevin C. "Observations of the directional spectrum of fetch-limited waves." *Journal of Physical Oceanography* Vol. 28 No. 3 (1998): pp. 495–512.

[23] Mj, Dripta, McAllister, Mark L, Bredmose, Henrik, Adcock, Thomas A A and Taylor, Paul H. "Harmonic structure of wave loads on a surface piercing column in directionally spread and unidirectional random seas." *Journal of Ocean Engineering and Marine Energy* (2023): pp. 1–19.

[24] Ding, H, Zang, J, Zhao, G, Tang, T, Taylor, P H, Adcock, T A A, Dai, S, Ning, D, Chen, L, Li, J and Wang, R. "Experimental Investigation of Nonlinear Forces on a Cylinder-Type Offshore Wind Turbine Foundation Under Different Wave Spreading Conditions." *43rd International Conference on Offshore Mechanics and Arctic Engineering, Singapore*. 2024.

[25] Gibbs, RH and Taylor, PH. "Formation of walls of water in 'fully'nonlinear simulations." *Applied Ocean Research* Vol. 27 No. 3 (2005): pp. 142–157.

[26] Adcock, Thomas A A, Gibbs, Richard H and Taylor, Paul H. "The nonlinear evolution and approximate scaling of directionally spread wave groups on deep water." *Proceedings of the Royal Society A: Mathematical, Physical and Engineering Sciences* Vol. 468 No. 2145 (2012): pp. 2704–2721.

[27] Latheef, M, Swan, C and Spinneken, J. "A laboratory study of nonlinear changes in the directionality of extreme seas." *Proceedings of the Royal Society A: Mathematical, Physical and Engineering Sciences* Vol. 473 No. 2199 (2017): p. 20160290.

[28] Tang, Tianning, Tromans, Peter S and Adcock, Thomas A A. "Field measurement of nonlinear changes to large gravity wave groups." *Journal of Fluid Mechanics* Vol. 873 (2019): pp. 1158–1178.

[29] DNV, GL. "DNVGL-ST-0126: Support structures for wind turbines." *Oslo, Norway: DNV GL* (2016).

[30] DNV, GL. "DNVGL-C203: Fatigue design of offshore steel structures." *Oslo, Norway: DNV GL* (2021).

[31] DNV, GL. "DNVGL-C202: Buckling strength of shells." *Oslo, Norway: DNV GL* (2019).

[32] EN, BS. "1 (2004). eurocode 7: Geotechnical design-part 1: General rules." *British Standards, UK* (1997).